Quantum Electronics **47** (5) 394–399 (2017)

https://doi.org/10.1070/QEL16350

Frequency standards based on ultracold atoms in tests of general relativity, navigation and gravimetry

K.Yu. Khabarova, K.S. Kudeyarov, N.N. Kolachevsky

Abstract. **Research and development in the field of optical clocks based on ultracold atoms and ions have enabled the relative uncertainty in frequency to be reduced down to a few parts in 10^{18}. The use of novel, precise frequency comparison methods opens up new possibilities for basic research (sensitive tests of general relativity, a search for a drift of fundamental constants and a search for 'dark matter') as well as for state-of-the-art navigation and gravimetry. We discuss the key methods that are used in creating precision clocks (including transportable clocks) based on ultracold atoms and ions and the feasibility of using them in resolving current relativistic gravimetry issues.**

Keywords: *ultracold atoms and ions, optical clock, general theory of relativity, relativistic gravimetry.*

1. Introduction

Proposed by Einstein in 1915, the basic equations of the theory of general relativity (TGR) relate the geometry of space–time to matter and its motion, treating gravity as the curvature of space–time. An essential role in the advent of the TGR was played by two key experiments: the Michelson–Morley experiment (1887), which proved that the speed of electromagnetic waves is isotropic and constant, and the Eotvos experiment (1890), which showed that the inertial and gravitational masses are equivalent. Immediately after its advent, gorgeous evidence was obtained in support of the TGR, which accounted for two effects: Mercury's perihelion shift (Einstein, Schwarzschild, 1915–1916) and the deflection of light by gravity (Eddington, 1919). One effect predicted by the TGR and not detected previously was the gravitational frequency shift and time dilation in a gravitational field. However, because of the almost complete lack of new observations and experiments up to the 1960s, many predictions of the TGR were put into question.

K.Yu. Khabarova, N.N. Kolachevsky P.N. Lebedev Physical Institute, Russian Academy of Sciences, Leninsky prosp. 53, 119991 Moscow, Russia; All-Russian Research Institute of Physicotechnical and Radiotechnical Measurements, 141570 Mendeleevo, Moscow region, Russia; Moscow Institute of Physics and Technology (State University), Institutskii per. 9, 141701 Dolgoprudnyi, Moscow region, Russia; e-mail: kolachevsky@lebedev.ru, kseniakhabarova@gmail.com;
K.S. Kudeyarov Moscow Institute of Physics and Technology (State University), Institutskii per. 9, 141701 Dolgoprudnyi, Moscow region, Russia; e-mail: kost1994@yandex.ru

Received 9 March 2017
Kvantovaya Elektronika **47** (5) 394–399 (2017)
Translated by O.M. Tsarev

The golden age of the TGR was marked with the discovery of pulsars in binary systems (Taylor, Hulse, 1976), which offered a unique possibility of observing the behaviour of natural millisecond clocks moving in a strong gravitational field, and with a number of ground-based experiments. The most important of them were the experiment performed by Hafele and Keating (1971), who compared precision caesium clocks that were flown around the world in opposite directions, and the Gravity Probe A experiment (1976). At present, the TGR is widely used in addressing astronomical and satellite navigation issues. Rapidly developing areas of research include the physics of strong gravitational fields, the physics of gravitational waves and a number of applied issues, which are addressed in this paper.

The consequences of the TGR include time dilation in a gravitational field and the gravitational frequency shift. Both effects are of the order of $\Delta U/c^2$ (where ΔU is the variation in gravitational potential) and can reach relative values of order 10^{-10} in near-Earth space. Accordingly, these effects should be taken into account in addressing navigation issues and synchronising clocks differing in altitude. In the case of standards with a relative signal frequency uncertainty in the range $\sim 10^{-14}$ to 10^{-15}, the gravitational effects can be taken into account by accurately measuring the height difference using classical levelling and ranging methods. Given that, near the Earth's surface, the height difference correction is just 10^{-16} m^{-1}, this approach is suitable for most applications.

Advances in frequency standards and comparison methods have made it possible to invert the problem, i.e. to accurately measure the gravitational potential difference and, accordingly, determine the height difference between objects on the Earth's surface. Researchers in the world's leading laboratories (in the United States, Japan and Germany) have created optical frequency standards with a relative frequency instability as low as a few parts in 10^{18} [1, 2]. There are transportable optical clocks based on ultracold atoms with a relative instability less than 10^{-16} (see Riehle [3] and references therein). A number of Russian scientific centres have also focused considerable effort on high-accuracy optical clocks: researchers at the All-Russia Research Institute of Physical and Radio Engineering Measurements (VNIIFTRI) aim to create an optical standard based on ultracold strontium atoms with a relative instability of 10^{-17}.

In a number of countries, researchers have demonstrated the possibility of comparing optical frequency standards using stabilised optical fibre communication links with a relative uncertainty at a level of 10^{-19} over distances up to 2000 km. In 2016, Deschênes et al. [4] demonstrated for the first time the possibility of optical clock comparison using open channels, in particular through a satellite. Such methods

enable optical clock comparison with a relative uncertainty of 10^{-18} at an averaging time near 1000 s. A European network is under construction which will include existing standards and communication channels [3].

The high accuracy and stability of novel frequency standards allow them to be utilised in gravimetry applications. Comparing two identical strontium clocks spaced 15 km apart and connected by an optical fibre link, Takano et al. [5] measured the relative height difference between them. The height difference was calculated using general relativity methods and was determined with an accuracy of 5 cm. Thus, a new method for height difference evaluation, capable of competing with the best classical geodesy methods, was demonstrated experimentally.

Comparison of identical frequency standards in a global network [3] allows gravitational potential differences to be determined on a continental scale with an uncertainty of the order of 1 cm. The first experiments have been carried out in the framework of the ITOC international project [6], aimed at resolving this issue.

Below, we present examples of how general relativity results are used for frequency standard comparison, describe advances in optical clock development and comparison and demonstrate the possibilities of determining the relativistic geoid using optical clocks.

2. General relativity effects in near-Earth space

Since the gravitational potential U is low near the Earth's surface, the space–time metric in an inertial, nonrotating frame of reference can be represented as

$$g_{00} = -\left(1 - \frac{2U}{c^2}\right), \quad g_{ij} = \left(1 + \frac{2U}{c^2}\right)\delta_{ij}, \tag{1}$$

differing from the Minkowski metric by the $2U/c^2$ terms (here, δ_{ij} is the Kronecker delta). The gravitational potential U is contributed by the Earth's potential U_E and the tidal potential U_T ($U = U_E + U_T$). Retaining only lower harmonics, we can represent the Earth's gravitational potential in the form

$$U_E = \frac{GM_E}{R} + J_2 GM_E \alpha_1 \frac{1 - \sin^2\theta}{2R^3} + \ldots, \tag{2}$$

where GM_E is the product of the gravitational constant with the Earth's mass and R is the distance to the Earth's centre. In this approximation, the Earth is an ellipsoid oblate along its axis due to its rotation, with a quadrupole coefficient J_2 and a semimajor axis a_1 (θ is its polar angle). On the Earth's surface, the gravitational potential is $U_E = 6.2\times10^7$ m^2 s^{-2}, and the tidal potential, due mainly to comparable contributions from the Sun and the Moon, is $U_T \sim 10^{-7}U_E$.

The surface of constant gravitational potential, with allowance for the centrifugal potential due to the Earth's rotation, is referred to as the Earth's geoid, which is close to but does not coincide with the surface of the world ocean. In the definition of the geoid, tidal effects are left out of account. The shape of the geoid can be calculated with allowance for gravitational anomalies and differs significantly from that of the surface of the continents. Precise determination of the surface of the geoid was the purpose of the Gravity Recovery and Climate Experiment (GRACE, 2002) space mission, whose operating principle was based on precision laser ranging of two low (500 km) earth orbit satellites spaced 200 km apart. This allows gravitational anomalies to be measured up to about the 120th spherical harmonic. The mean error of determination of the geoid from GRACE data is slightly less than 1 cm [7]. The shape of the geoid can be more accurately determined using gravity (g) maps. It is important to note that global navigation satellite systems (GNSS's) make it possible to determine the height relative to a reference geocentric ellipsoid, which does not coincide with the geoid.

The consequences of the TGR include a frequency shift of electromagnetic waves and time dilation in a gravitational field. Using (1), we can find that, when a wave propagates in a gravitational field, its frequency varies as

$$\nu' = \nu\left(1 + \frac{U' - U}{c^2}\right), \tag{3}$$

i.e. the frequency of the wave increases as the centre of gravity is approached. In turn, time slows down near massive bodies:

$$t' = t\left(1 - \frac{U' - U}{c^2}\right). \tag{4}$$

At the beginning of the development of the TGR, experimental verification of these effects was impossible because of the relatively low measurement accuracy and the influence of motion of bodies (Doppler effect, time dilation and Sagnac effect).

One of the most accurate measurements aimed at verifying the general relativity effects (3) and (4) was performed using an active hydrogen maser in the Gravity Probe A suborbital spacecraft launched in 1976 upward to about 10 000 km, whose frequency was compared to that of a ground-based standard [8]. Possible deviations from (3) and (4) were tested at a level of 7×10^{-5} relative, which is still one of the most sensitive tests of the equivalence principle. Relation (3) can be obtained by considering 'Einstein's lift', which suggests that the effect of gravity and the Doppler shift are equivalent in the Newtonian approximation.

In astrophysics, the time dilation effect (Shapiro time delay) is observed e.g. in timing pulsars in binary star systems. A pulsed pulsar signal passing near the gravitational field of the pulsar companion slows down, which leads to a well-observed time dilation effect, at a level of tens of microseconds [9].

Relations (3) and (4) are widely used in practice as well. Among space applications, it is worth mentioning the operation of GNSS satellite systems (GLONASS, GPS and others), which orbit at an altitude near 20 000 km. Since the basic principle of the GNSS's is to compare the time signal of an on-board clock to that of a ground-based clock, it is necessary to make a frequency correction related to gravitational effects and the motion of the satellites (time dilation). The two effects are comparable in magnitude and opposite in sign [10]. To synchronise the on-board and ground-based clocks, a correction of -4.5×10^{-10} relative is introduced into the on-board system (Fig. 1).

Another example is the RadioAstron radio telescope [P.N. Lebedev Physical Institute (LPI), Russian Academy of Sciences (RAN)], a functioning space laboratory with an active hydrogen maser on board. Since the satellite has a highly elongated elliptical orbit, the gravitational effect of the Earth's field varies with time. After compensation for the Doppler effect, the observed frequency shift due to the gravi-

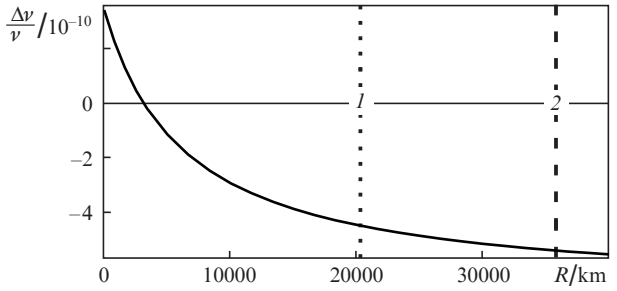

Figure 1. Frequency correction of a standard in a circular-orbit satellite for synchronisation with an observer on the Earth's surface vs. satellite orbit altitude R_{orb}: (*1*) GNSS and (*2*) geostationary satellite orbits.

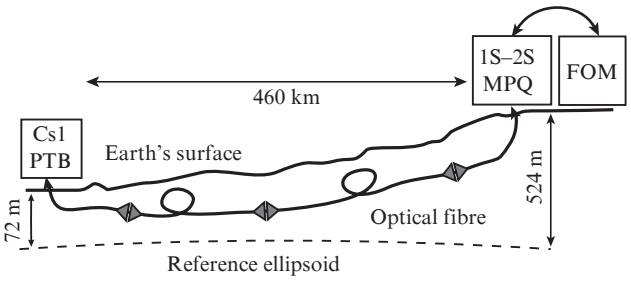

Figure 2. Schematic of comparison of the frequency of the 1S–2S optical transition in atomic hydrogen (MPQ) with the frequency of the FOM transportable caesium primary standard and with that of the Cs1 remote fountain (PTB) using a 920-km optical fibre link. In the case of comparison with the Cs1 signal, the gravitational frequency shift due to the height difference between MPQ and PTB, 4.4×10^{-14}, was taken into account. The results of the two measurements of the absolute frequency, MPQ–FOM [13] and MPQ–PTB [14], coincided to within 5×10^{-15}.

tational field is up to 3 Hz at a carrier frequency of 8.4 GHz. High-accuracy phase comparisons with ground-based frequency standards are expected to ensure verification of relation (4) with a sensitivity of 2.5×10^{-5} [11], which improves the accuracy of the GPA mission result [8].

Changes in clock rate are also observed in the case of comparison of ground-based standards. Given that the relative uncertainty of caesium fountain primary frequency standards approaches 2×10^{-16} [12], comparison between such standards requires knowledge of relative heights to within 1 m. Given that the Earth's surface has height differences up to several thousand metres, the time correction (4) is indispensable in the case of remote comparison between standards (using duplex communication, GNSS's, optical fibre links etc.).

As an example, note one of the first precise optical frequency measurements performed for the hydrogen 1S–2S transition relative to the frequency of a remote caesium fountain by a joint team from the Max Planck Institute for Quantum Optics (MPQ), LPI and the National Metrology Institute of Germany (PTB) [13]. Previous measurements [14] were made using the FOM transportable caesium fountain, which was generously provided by the LNE-SYRTHE laboratory. In 2012, a 920-km optical fibre link was made between PTB and MPQ (the straight-line distance between PTB and MPQ is 460 km), which enabled precision comparisons in the optical and radio frequency ranges [15]. This opened up the possibility of measuring the 1S–2S frequency in atomic hydrogen relative to a PTB national primary standard: Cs1 caesium fountain. In those measurements, it was necessary to take into account the height difference between PTB (Braunschweig) and MPQ (Munich), which is 452 m (Fig. 2), and make the corresponding frequency shift correction: 4.4×10^{-14}. The frequency of the transition in atomic hydrogen was determined with an uncertainty of 11 Hz (fractional uncertainty of 4.5×10^{-15}). The absolute frequency obtained coincided to within experimental uncertainty with the result of a previous measurement [14], performed using the FOM mobile fountain.

In recent years, a number of more accurate comparisons between remote standards were performed, including an optical clock comparison with a measurement uncertainty of 5×10^{-17}. The existing geodesic methods still have sufficient accuracy for such comparisons and allow the relativistic correction (4) to be made using information about the height difference and, accordingly, about the gravitational potential difference, with no significant effect on the uncertainty budget. At the same time, achieving accuracy better than 10^{-17} requires knowledge of the relative height of the clock with an accuracy better than 10 cm, which is a serious problem in the case of a remote clock. On the other hand, a possibility emerges for inverting the problem and using identical precision clocks for determining gravitational potential and height differences [16].

3. Optical clocks with a frequency uncertainty below 10^{-17} and comparison methods for such clocks

The past few years have seen the advent of a number of stationary optical clocks with a frequency uncertainty below 10^{-17}. These include clocks based on neutral atoms in optical lattices (see e.g. Refs [1, 2]) and single-ion clocks (see e.g. Refs [17, 18]). A detailed review of optical clocks was presented by Ludlow et al. [19]. At short times of order 1 s, the relative instability of such clocks is determined by the spectral characteristics of the laser system used to excite the transition and can be as low as 10^{-16} [20]. The laser frequency is then actively stabilised to the transmission peak of an ultrastable optical cavity. At longer times, laser frequency stability is determined by the frequency of a transition in a laser-cooled atom or ion. Optical lattice clocks [1, 2] demonstrate better relative instability characteristics owing to the larger number of atoms interacting with light. A typical relative instability of the best optical lattice clocks depends on the averaging time τ (in seconds) as $5\times10^{-16}(\tau/\text{s})^{-1/2}$ [2], which allows the 10^{-18} uncertainty level to be reached by averaging over several hours. Ion standards have somewhat lower stability, but they are comparable in accuracy with neutral-atom standards, because a single ion in a Paul trap has a weak response to external disturbances. Moreover, ion traps are compact (no greater than 1 dm^3 in volume) and less sensitive to the settings of the cooling and interrogating fields.

In Russia, researchers aim to create an optical clock based on ultracold strontium atoms with a relative frequency uncertainty at a level of 10^{-17} (VNIIFTRI) [21]. Considerable effort has also been focused on optical clocks based on single ions of ytterbium [Institute of Laser Physics (ILP), Siberian Branch, RAN] [22] and aluminium (LPI) [23] and neutral thulium atoms (LPI) [24].

As seen in Fig. 3, the methods used to compare remote microwave frequency standards (duplex and GNSS) are incapable of comparing optical frequency standards with an accu-

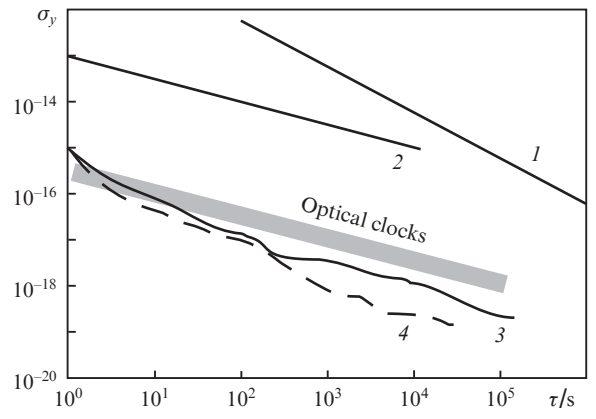

Figure 3. Relative instability (Allan deviation σ_y) due to different transmission channels of the signals used for comparing standards: (*1*) comparison using a GNSS (carrier phase), (*2*) duplex (TWSTFT), (*3*) long optical fibre (over 1000 km) with the use of the carrier phase, (*4*) optical satellite channel (carrier phase). The shaded band represents typical characteristics of the best optical clocks based on lattice-trapped neutral atoms.

racy better than 10^{-16}. This is the consequence of atmospheric fluctuations, delays and the long time required for signal acquisition.

A number of methods have been proposed and implemented for synchronisation with the use of actively stabilised optical fibres. Examples of frequency synchronisation on a continental scale can be found in Refs [15, 19]. Active stabilisation and information transmission methods that utilise the phase of the optical carrier ensure instability at a level of a few parts in 10^{19} [Fig. 3, curve (*3*)]. This proves to be sufficient for optical clock comparison with no loss of accuracy. The network of optical fibre communication links between the leading European metrological centres is constantly growing. Use is made of both dedicated and ordinary Internet accesses with proper modifications. This research direction has recently been the subject of a review [25].

Another possibility is to compare optical standards using an open channel, through a satellite. The operating principle is similar to signal comparison using an optical fibre, which allows the number of intermediate amplifier stations to be reduced. The first experimental efforts in this direction [4] show that open-channel comparisons are not inferior in performance to optical-fibre comparisons. It should be noted, however, that the method may turn out to be rather sensitive to ambient conditions and has not yet been tested using satellite communications.

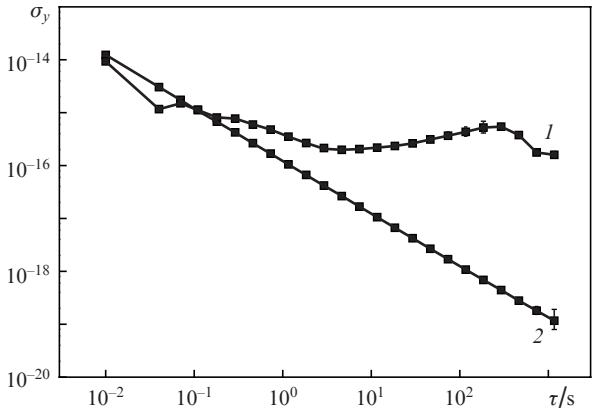

Figure 4. Relative instability in terms of Allan deviation σ_y due to a short (30 m) optical fibre communication link: (*1*) without active stabilisation, (*2*) actively stabilised link.

Researchers at LPI aim to create a stabilised optical fibre link using information about the phase of the optical carrier. Using a short link 30 m in length as an example, they showed that, in the case of active stabilisation, frequency instability was as low as 10^{-19} over a period of 1000 s (Fig. 4). Currently, they investigate characteristics of signal transmission through a long (4 km) optical fibre using frequency-stabilised laser light. It is seen from Fig. 4 that the performance achieved to date compares well to the best results so far in the world. Similar studies are under way at ILP.

4. Transportable optical frequency standards

An alternative approach to frequency comparison and the verification of various frequency standards is to employ transportable standards. FOM, the only transportable caesium fountain [26], was used in a wide range of international comparisons and tests of fundamental theories and has completely justified its existence. The development of transportable systems is undoubtedly a more complex problem than that of stationary clocks, because it requires compact solutions, high reliability, mechanical stability and stability to external disturbances.

To date, several transportable optical standards surpassing the FOM fountain in performance have been demonstrated. In particular, researchers at PTB created and characterised a transportable optical standard (several cubic metres in volume) based on ultracold strontium atoms in an optical lattice [27]. The standard can be placed in a closed-top automobile trailer. At a rated frequency instability of $1.3\times 10^{-15}(\tau/\mathrm{s})^{-1/2}$, the standard has a frequency uncertainty of 7×10^{-17}. In the framework of the ITOC project, it was compared to a remote primary frequency standard [6].

Researchers in China created and characterised a compact transportable Ca^+ standard [28]. It has a modular design and its volume is about 1 m^3. In spite of its poorer instability, $2.3\times 10^{-14}(\tau/\mathrm{s})^{-1/2}$, it is comparable in accuracy (7.7×10^{-17}) to the PTB strontium standard.

Transportable optical standards with an accuracy better than 10^{-16} (the limit achievable with caesium fountains) are under development in a number of countries and are intended for several purposes, one of which is to develop a synchronised optical clock network and a model of a relativistic geoid. Moreover, a modular configuration and high compactness of proposed models are an important step on the way to on-board space-based optical standards. Note that a number of successful suborbital launches have already been performed: in 2015 a femtosecond optical frequency comb stabilised to a rubidium frequency standard was launched [29], and in January 2017 a Bose–Einstein condensate was produced for the first time on board a spacecraft (MAIUS-1 project) [30]. This points to high technological readiness to produce precise optical clocks on the Earth's orbit, which will allow the accuracy of time and frequency signal synchronisation between orbital groups to be improved by orders of magnitude and open up additional possibilities for resolving relativistic geodesy issues.

5. Potential applications in relativistic geodesy

The gravitational time dilation effect was demonstrated for the first time using an atomic clock under laboratory conditions by comparing two identical optical clocks based on single aluminium ions [31]. During the experiment, one vacuum chamber with an ion was 33 cm above the other, which led to a relative frequency shift of $(4.1 \pm 1.6) \times 10^{-17}$. The experiment laid the foundation of a new practical direction based on precise frequency standards: relativistic geodesy. Clearly, given the levelling accuracy reached to date and the accuracy in determining the geoid and reference ellipsoid (a few centimetres), serious competition with the above methods is only possible at a clock accuracy at a level of a few parts in 10^{18}.

The method builds on the definition of the geoid as an equipotential surface with a potential U_0 (Fig. 5). According to relation (4), clocks located on this surface will tell the same time. Thus, having a set of precision clocks and comparison channels, one can reconstruct the shape of the geoid, obtaining a so-called relativistic geoid. Accordingly, the height H relative to the geoid can be measured using the relation

$$H = \frac{U - U_0}{g}, \tag{5}$$

where g is the acceleration of gravity at the point of interest. One obvious advantage of this approach is the possibility of directly determining the gravitational potential, with no need to integrate g over the trajectory of motion. Even though g can be measured with a relative uncertainty down to a few microgals, integration leads to considerable error propagation. The same refers to levelling methods, in which uncertainty grows roughly as the square root of the distance between points. In addition, clock comparison requires a much shorter integration time (10^3 to 10^4 s) and can be used to investigate dynamic processes, whereas the existing gravity maps are essentially static.

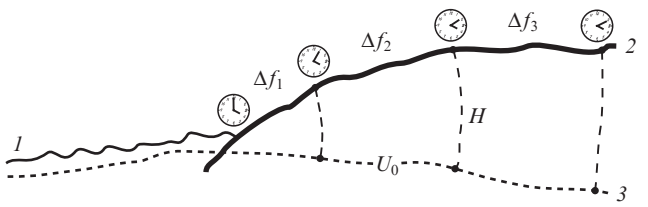

Figure 5. Method for direct determination of the orthometric height H using precision clocks: (*1*) ocean surface, (*2*) land surface, (*3*) surface of a geoid with a constant gravitational potential U_0.

One important step towards the development of relativistic geodesy methods with the use of optical clocks is the experiment carried out in 2015 in Japan by the Katori group [5]. They compared several cryogenic optical clocks based on strontium atoms in an optical lattice: clocks at the Tokyo University and the Metrological Institute, RIKEN, spaced 15 km apart. The institutes differed in altitude by about 15 m. Given that the relative accuracy of the clocks was 4×10^{-18} and that the optical fibre communication link produced no additional uncertainty, it was found that the gravitational potential difference was -148.55 ± 0.53 m^2 s^{-2}. This corresponds to a 5-cm uncertainty in height difference. The measurement result obtained using clocks coincided with a result obtained using levelling (-148.14 ± 0.06 m^2 s^{-2}). The higher accuracy of the levelling method is here due to the relatively small separation between the clocks.

Levelling is incapable of monitoring dynamic changes in potential, which can be caused e.g. by the Earth's crust displacements. At the accuracy reached to date, tidal potentials are essential. Their effect was analysed in detail by Voigt et al. [32]. It increases with increasing distance between the clocks being compared.

6. Conclusions

As a result of intense research in the past decade towards the development of optical clocks, reaching relative frequency uncertainty at a level of one part in 10^{17} became essentially a technical problem. Clearly, resolving this problem requires intense work of experts and considerable resources. Comparison of remote standards with the use of optical fibre links also became a technical problem. Researchers in Europe actively develop a network of optical and microwave standards [6]. Its key goals are to produce a time scale with uncertainty at a level of 10^{-17} and, as consequence, to begin work aimed at formulating the concept of relativistic geoid. The latter will become an important supplement to the existing geodesic methods and, possibly, will soon compete with them.

To extend the capabilities of the network, a number of transportable standards have been created to date. Their accuracy has surpassed a few parts in 10^{16} and continues to improve. Optical clocks were used to experimentally demonstrate the capabilities of chronometric geodesy, which allows height differences to be determined with 5-cm uncertainty. Researchers in Europe performed a number of key test experiments on board of spacecrafts, which opened up the possibility of launching optical clocks to the Earth's orbit. Unfortunately, no work on the creation of a transportable standard or on-board apparatus elements has been begun in Russia.

In a close-up perspective, precise optical clocks on board of a spacecraft on an accurately determined orbit can extend navigation capabilities for both improving GNSS synchronisation and producing a reference orbit for accurate gravitational potential measurements.

Acknowledgements. This work was supported by the Russian Science Foundation (Grant No. 16-00096).

References

1. Schioppo M., Brown R.C., McGrew W.F., Hinkley N., Fasano R.J., Beloy K., Yoon T.H., Milani G., Nicolodi D., Sherman J.A., Phillips N.B., Oates C.W., Ludlow A.D. *Nat. Photonics*, **11**, 48 (2017).
2. Ushijima I., Takamoto M., Das M., Ohkubo T., Katori H. *Nat. Photonics*, **9**, 185 (2015).
3. Riehle F. *Nat. Photonics*, **11**, 25 (2017).
4. Deschênes J.-D., Sinclair L.C., Giorgetta F.R., Swann W.C., Baumann E., Bergeron H., Cermak M., Coddington I., Newbury N.R. *Phys. Rev. X*, **6**, 021016 (2016).
5. Takano T., Takamoto M., Ushijima I., Ohmae N., Akatsuka T., Yamaguchi A., Kuroishi Y., Munekane H., Miyahara B., Katori H. *Nat. Photonics*, **10**, 662 (2016).
6. http://projects.npl.co.uk/itoc/project-structure/reg/gravity-potential.
7. Tapley B., Ries J., Bettadpur S., Chambers D., Cheng M., Condi F., Gunter B., Kang Z., Nagel P., Pastor R., Pekker T., Poole S., Wang F. *J. Geod.*, **79**, 467 (2005).

8. Vessot R.F.C., Levine M.W., Mattison E.M., Blomberg E.L., Hoffman T.E., Nystrom G.U., Farrel B.F., Decher R., Eby P.B., Baugher C.R., Watts J.W., Teuber D.L., Wills F.D. *Phys. Rev. Lett.*, **45**, 2081 (1980).
9. Kramer M., Stairs I.H., Manchester R.N., McLaughlin M.A., Lyne A.G., Ferdman R.D., Burgay M., Lorimer D.R., Possenti A., D'Amico N., Sarkissian J.M., Hobbs G.B., Reynolds J.E., Freire P.C.C., Camilo F. *Science*, **314**, 97 (2006).
10. Riehle F. *Frequency Standards: Basics and Applications* (New York: Wiley, 2005; Moscow: Fizmatlit, 2009).
11. Biryukov A.V., Kauts V.L., Kulagin V.V., Litvinov D.A., Rudenko V.N. *Astronom. Zh.*, **91**, 887 (2014).
12. Levi F., Calonico D., Calosso C.E., Godone A., Micalizio S., Costanzo G.A. *Metrologia*, **51**, 270 (2014).
13. Matveev A., Parthey C.G., Predehl K., Alnis J., Beyer A., Holzwarth R., Udem Th., Wilken T., Kolachevsky N., Abgrall M., Rovera D., Salomon C., Laurent P., Grosche G., Terra O., Legero T., Schnatz H., Weyers S., Altschul B., Hänsch T.W. *Phys. Rev. Lett.*, **110**, 230801 (2013).
14. Parthey C. G., Matveev A., Alnis J., Bernhardt B., Beyer A., Holzwarth R., Maistrou A., Pohl R., Predehl K., Udem Th., Wilken T., Kolachevsky N., Abgrall M., Rovera D., Salomon C., Laurent P., Hänsch T.W. *Phys. Rev. Lett.*, **107**, 203001 (2011).
15. Predehl K., Grosche G., Raupach S.M.F., Droste S., Terra O., Alnis J., Legero T., Hänsch T.W., Udem Th., Holzwarth R., Schnatz H. *Science*, **336**, 441 (2012).
16. Lisdat C., Grosche G., Quintin N., Shi C., Raupach S.M.F., Grebing C., Nicolodi D., Stefani F., Al-Masoudi A., Dörscher S., Häfner S., Robyr J.-L., Chiodo N., Bilicki S., Bookjans E., Koczwara A., Koke S., Kuhl A., Wiotte F., Meynadier F., Camisard E., Abgrall M., Lours M., Legero T., Schnatz H., Sterr U., Denker H., Chardonnet C., Le Coq Y., Santarelli G., Amy-Klein A., Le Targat R., Lodewyck J., Lopez O., Pottie P.-E. *Nat. Commun.*, **7**, 12443 (2016).
17. Chou C.W., Hume D.B., Koelemeij J., Wineland D.J., Rosenband T. *Phys. Rev. Lett.*, **104**, 070802 (2010).
18. Huntemann N., Sanner C., Lipphardt B., Tamm Chr., Peik E. *Phys. Rev. Lett.*, **116**, 063001 (2016).
19. Ludlow A.D., Boyd M.M., Ye J., Peik E., Schmidt P.O. *Rev. Mod. Phys.*, **87**, 637 (2015).
20. Matei D.G., Legero T., Häfner S., Grebing C., Weyrich R., Zhang W., Sonderhouse L., Robinson J.M., Ye J., Riehle F., Sterr U. arXiv:1702.04669.
21. Khabarova K.Yu., Galyshev A.A., Strelkin S.A., Kostin A.S., Belotelov G.S., Berdasov O.I., Gribov A.Yu., Kolachevsky N.N., Slyusarev S.N. *Quantum Electron.*, **45**, 166 (2015) [*Kvantovaya Elektron.*, **45**, 166 (2015)].
22. Chepurov S.V., Lugovoi A.A., Kuznetsov S.N. *Quantum Electron.*, **44**, 527 (2014) [*Kvantovaya Elektron.*, **44**, 527 (2014)].
23. Semerikov I.A., Zalivako I.V., Shpakovskii T.V., Borisenko A.S., Khabarova K.Yu., Kolachevsky N.N. *Quantum Electron.*, **46**, 935 (2016) [*Kvantovaya Elektron.*, **46**, 935 (2016)].
24. Sukachev D., Fedorov S., Tolstikhina I., Tregubov D., Kalganova E., Vishnyakova G., Golovizin A., Kolachevsky N., Khabarova K., Sorokin V. *Phys. Rev. A*, **94**, 022512 (2016).
25. Khabarova K.Yu., Kalganova E.S., Kolachevsky N.N. *Usp. Fiz. Nauk*, 2017 (in press).
26. Vian C., Rosenbusch P., Marion H., Bize S., Cacciapuoti L., Zhang S., Abgrall M., Chambon D., Maksimovic I., Laurent P., Santarelli G., Clairon A., Luiten A., Tobar M., Salomon C. *IEEE Trans. Instrum. Meas.*, **54**, 833 (2005).
27. Koller S.B., Grotti J., Vogt St., Al-Masoudi A., Dörscher S., Häfner S., Sterr U., Lisdat Ch. *Phys. Rev. Lett.*, **118**, 073601 (2017).
28. Cao J., Zhang P., Shang J., Cui K., Yuan J., Chao S., Wang S., Shu H., Huangar X. arXiv:1607.03731.
29. Lezius M., Wilken T., Deutsch C., Giunta M., Mandel O., Thaller A., Schkolnik V., Schiemangk M., Dinkelaker A., Kohfeldt A., Wicht A., Krutzik M., Peters A., Hellmig O., Duncker H., Sengstock K., Windpassinger P., Lampmann K., Hülsing T., Hänsch T.W., Holzwarth R. *Optica*, **3**, 1381 (2016).
30. http://www.sscspace.com/missions-projects/ongoing/maius-1.
31. Chou C., Hume D., Rosenband T., Wineland D. *Science*, **329**, 1630 (2010).
32. Voigt C., Denker H., Timmen L. *Metrologia*, **53**, 1365 (2016).